Research Article

Ngoc Duc Vu*, Duong Thi Ngoc Diep, Nhat An Nguyen, Huynh Bao Long, Binh An Pham*

Physicochemical components, antioxidant activity, and predictive models for quality of soursop tea (*Annona muricata* L.) during heat pump drying

https://doi.org/10.1515/chem-2024-0095
received July 10, 2024; accepted September 12, 2024

Abstract: The peel and pulp of soursop are ideal for creating a new tea product, offering a unique flavor compared to traditional leaf tea. This study develops mathematical models to describe the drying process, decomposition of bioactive components, and antioxidant activity of soursop slices. The slices were dried at four temperatures (20–50°C) using industrial-scale heat pump drying. Changes in moisture ratio (MR) were calculated and compared with 30 previous models. Additionally, two and four mathematical models were used to analyze data on total flavonoid content (TFC) and antioxidant activity. The model fits were evaluated based on statistical parameters (R^2, root mean square error, χ^2). The results indicated that the drying process at 20°C involved two mechanisms following the Aghbashlo model ($R^2 > 0.993$). At higher temperatures, the moisture removal process followed a single mechanism. Zero order, first order, and polynomial quadratic models were suitable for describing TFC decomposition and antioxidant activity, depending on the temperature. The activation energy of MR (29.89 kJ/mol) was lower than that of 2,2′–azino-bis–3–ethylbenzothiazoline–6–sulfonic acid (37.02 kJ/mol) and 2,2–diphenyl–1-1-picrylhydrazyl (32.12 kJ/mol), indicating drying efficiency and retention of bioactive components. The study's findings are expected to enhance quality, improve economic efficiency, and expand the market for soursop tea.

Keywords: antioxidant activity, flavonoid degradation, heat pump drying, mathematical modeling, soursop drying kinetics

1 Introduction

Soursop tea made from the pulp and peel is a new product in Vietnam and rare internationally. Most soursop teas are typically made from leaves. The importance of this tea has increased due to its long shelf life and health benefits from bioactive compounds like polyphenols, flavonoids, and vitamins C and B1–B6 [1–3]. These components boost antioxidants, protect the liver, counteract toxins, and improve wound healing [4–6], and prevent diseases like cancer, cardiovascular diseases, and infections [7–11]. Additionally, rich minerals like Ca, Mg, P, K, Na, and Zn have been found. Tea made from the pulp and peel offers a unique flavor and experience, different from traditional leaf tea. It also reduces the pressure on harvesting leaves, protecting the plants and conserving natural resources. Moreover, previous studies on selecting soursop promise high-nutrient products favored by consumers [12–14].

Diversifying and developing high-quality soursop products is a key goal for Vietnam's agriculture and other major growing countries like Malaysia (1470.4 tons/year/356.7 ha) [15] and Nayarit (21860.02 tons/year) [7]. Vietnam's annual soursop yield is very high, averaging around 16–17 tons/ha [7]. This leads to spoilage due to short shelf life, causing waste and reducing agricultural economic efficiency [16]. Producing soursop tea in high-yield countries helps minimize spoilage and reduces the pressure of fresh fruit trade [17]. Countries with lower soursop yields will rely less on imports. Developing new soursop tea products from the peel and pulp also creates job opportunities for

* **Corresponding author: Ngoc Duc Vu**, Institute of Applied Technology and Sustainable Development, Nguyen Tat Thanh University, Ho Chi Minh City, 700000, Vietnam; Faculty of Chemical Engineering and Food Technology, Nong Lam University, Ho Chi Minh City, 700000, Vietnam, e-mail: vdngoc@ntt.edu.vn
* **Corresponding author: Binh An Pham**, Institute of Applied Technology and Sustainable Development, Nguyen Tat Thanh University, Ho Chi Minh City, 700000, Vietnam, e-mail: pban@ntt.edu.vn
Duong Thi Ngoc Diep, Nhat An Nguyen: Faculty of Chemical Engineering and Food Technology, Nong Lam University, Ho Chi Minh City, 700000, Vietnam
Huynh Bao Long: Faculty of Chemical Technology, Ho Chi Minh City University of Industry and Trade, Ho Chi Minh City, 700000, Vietnam

Open Access. © 2024 the author(s), published by De Gruyter. This work is licensed under the Creative Commons Attribution 4.0 International License.

farmers by boosting fruit processing and cultivation, enhancing the agricultural economy.

Besides the potential and challenges related to soursop, one crucial factor in processing soursop tea is the appropriate drying conditions. As product demand increases, drying equipment and methods need to be upgraded to meet the demand. However, industrial drying equipment is typically larger, includes upgraded components, and is more challenging to control than laboratory-scale dryers. Therefore, establishing a database to standardize the drying process and predict product quality is necessary. Identifying bioactive components (total flavonoids content [TFC]), antioxidant activity (2,2-diphenyl-1-1 picrylhydrazyl [DPPH] and 2,2′-azino-bis-3-ethylbenzothiazoline-6-sulfonic acid [ABTS]), and their relationship with moisture content (MC) allows for predicting product quality over time and improving dryer design [18]. The kinetic models provide a solid foundation for optimizing parameters in the drying process, aiming to enhance product quality and guide the production of soursop tea. Furthermore, these models have the potential to be integrated with advanced technological devices to establish a highly efficient automated system, allowing real-time monitoring of the drying process [19]. In addition to being applied to the drying kinetics of soursop, these models can also be used to relatively predict the quality of products from other similar materials.

Among the common drying methods for various materials, heat pump drying is considered to meet both the economic and product quality aspects, as it allows drying at low temperatures. However, research on this method is still limited [20]. Mathematical models of the drying process contribute to predicting quality and MC, serving as a basis for balancing economics, quality, and designing suitable drying equipment [21]. Existing reports on the mathematical modeling of thin-layer drying for fruits like mango [22], lemon [23], and golden apple [24] are mostly done on laboratory-scale equipment using convective hot air drying. Heat pump drying of mango slices has been reported [25]. However, mathematical modeling of soursop slice drying, including MC, TFC, and antioxidant activity (DPPH and ABTS), has not been reported. The aim of this study is to develop models describing changes in MC, TFC, and antioxidant activity (DPPH and ABTS) using experimental data from industrial-scale heat pump drying.

This work presents three new aspects not previously addressed in mathematical modeling of soursop slice drying kinetics on an industrial scale. First, the drying process was conducted at temperatures ranging from 20 to 50°C until the moisture ratio (MR) was less than 0.02 kg water/kg solid, monitoring key components such as MC, TFC, DPPH, and ABTS throughout. Second, a total of 30, 02, and 04 mathematical models were applied, respectively, to the processes of moisture removal, TFC degradation, and antioxidant activity reduction. The most suitable models were identified for soursop slice drying based on calculated kinetic parameters (coefficient of determination [R^2], chi-square [χ^2], rate constant [k], and root mean square error [RMSE]). Finally, the activation energy (E_a) for the drying process was determined for all parameters. The study findings are expected to enhance soursop tea production efficiency in the future. The current models can also serve as a reference for the drying process of various plants that possess high antioxidant activity and properties similar to soursop, such as *Sida acuta* [26]. Additionally, the proposal to combine soursop tea with caffeine represents a comprehensive development in enhancing the antioxidant capacity of the product [27].

2 Material and methods

2.1 Plant material

This study employed soursop fruit sourced from Tan Phu Dong, Tien Giang province, Vietnam (coordinates 10°14′43″ N 106°41′54″E). The fruits were harvested approximately 3 months after formation. Post-harvest, the fruits were stored at a temperature of 30 ± 2°C and promptly transported to Nguyen Tat Thanh within a maximum of 4 h for immediate study. The fruits weighed between 1.5 and 2 kg, featuring white pulp and a fresh green peel, and was free from bruising, waterlogging, or any damage [28]. Additionally, pesticide residues (Amitrole, Bifenazate, Clothianidin, Glufosinate-Ammonium) were tested and found to be below the permissible limits according to Vietnam's national food safety standards.

2.2 Drying procedure and heat pump dryer set-up

For each experiment, around 70 kg of fresh soursop, meeting the criteria in Section 2.1 (Figure 1a), were washed with water compliant with Vietnamese health standards. The soursop was manually cut lengthwise into 1–2 cm thick slices (Figure 1b), deseeded, and further sliced to 1–2 mm thickness (Figure 1c) (Diep Ky company, Ho Chi Minh City, Vietnam).

An industrial-scale heat pump dryer with a maximum capacity of 40 kg per batch of soursop (Figure 2) was utilized in the experiments. Each drying tray, measuring 47 × 55 × 2 cm (hole size: 0.5 × 0.5 cm), held 2.00 ± 0.10 kg of soursop slices (Figure 1). The dryer operated by drawing moist air from the medium (30 ± 2°C, relative humidity

Figure 1: Fresh soursop (a) was cut longitudinally (b) and then into thin slices (c).

[RH] = 78 ± 2%) and condensing the moisture using a 2 HP cooling system. The resulting low-humidity air (RH = 10 ± 2%), was measured using an absolute humidity analyzer (TP152, ThermoPro, China), was heated with an electric resistor to reach an air temperature of 20–50°C. This heated air was then circulated into the drying chamber as the drying agent to remove moisture.

The soursop was dried at 20, 30, 40, and 50°C (Airflow speed: 2.5 m/s) until the MC stabilized over three consecutive measurements, then the drying process was stopped. The MC, TFC, and ABTS and DPPH antioxidant activity were recorded every 15 min during drying. A balance (Dragon equipment, Ho Chi Minh City, Vietnam) and a heat-resistant camera (M500, 70MAI, Xiaomi, China) were installed to monitor MC throughout the drying process. Experimental data and previous mathematical models were used to develop models describing the changes in components (MC, TFC, ABTS, and DPPH antioxidant activity) during industrial-scale heat pump drying. Kinetic parameters, diffusion coefficients, and E_a were calculated.

2.3 Equipment and chemicals

Slicing equipment (Diep Ky company, Ho Chi Minh city, Vietnam) (Capacity: 80 kg of soursop per hour, motor: 0.5 HP, total blades: 2). Heat pump drying equipment (parameters depicted in Figure 2): Total number of drying trays: 20, airflow direction: from left to right, total electric resistor: 2, limited temperature: 20–50°C, and limited airflow speed: 0–5 m/s.

Aluminum chloride (97%, Merck), Potassium acetate (98.14%, Merck), ABTS (>98%, Merck), DPPH (95%, Merck).

2.4 Analytical methods

2.4.1 MC, drying rate (DR), and MR

A heat-resistant weighing device (Dragon equipment, Ho Chi Minh City, Vietnam) continuously weighs a drying tray with 2.00 ± 0.10 kg of material in a heat pump dryer. The MC of soursop slices is monitored and recorded every 15 min using a heat-resistant camera (M500, Xiaomi, China).

MC at the time t (kg/kg):

$$\mathrm{MC}_t = \frac{m_t - m_0 \times (100 - \mathrm{MC}_0)}{m_t}, \quad (1)$$

DR (kg/kg/min):

$$\mathrm{DR} = \frac{\mathrm{MC}_t - \mathrm{MC}_{t+\Delta t}}{\Delta t}, \quad (2)$$

MR (kg/kg):

$$\mathrm{MR} = \frac{\mathrm{MC}_t - \mathrm{MC}_{\mathrm{eq}}}{\mathrm{MC}_0 - \mathrm{MC}_{\mathrm{eq}}}, \quad (3)$$

where m_0: initial total weight of drying material (kg); m_t: total weight of drying material at time t (kg); MC_0, MC_t, and $\mathrm{MC}_{\mathrm{eq}}$ are initial MC (fresh soursop), MC at time t, and equilibrium MC, respectively (kg water/kg solid).

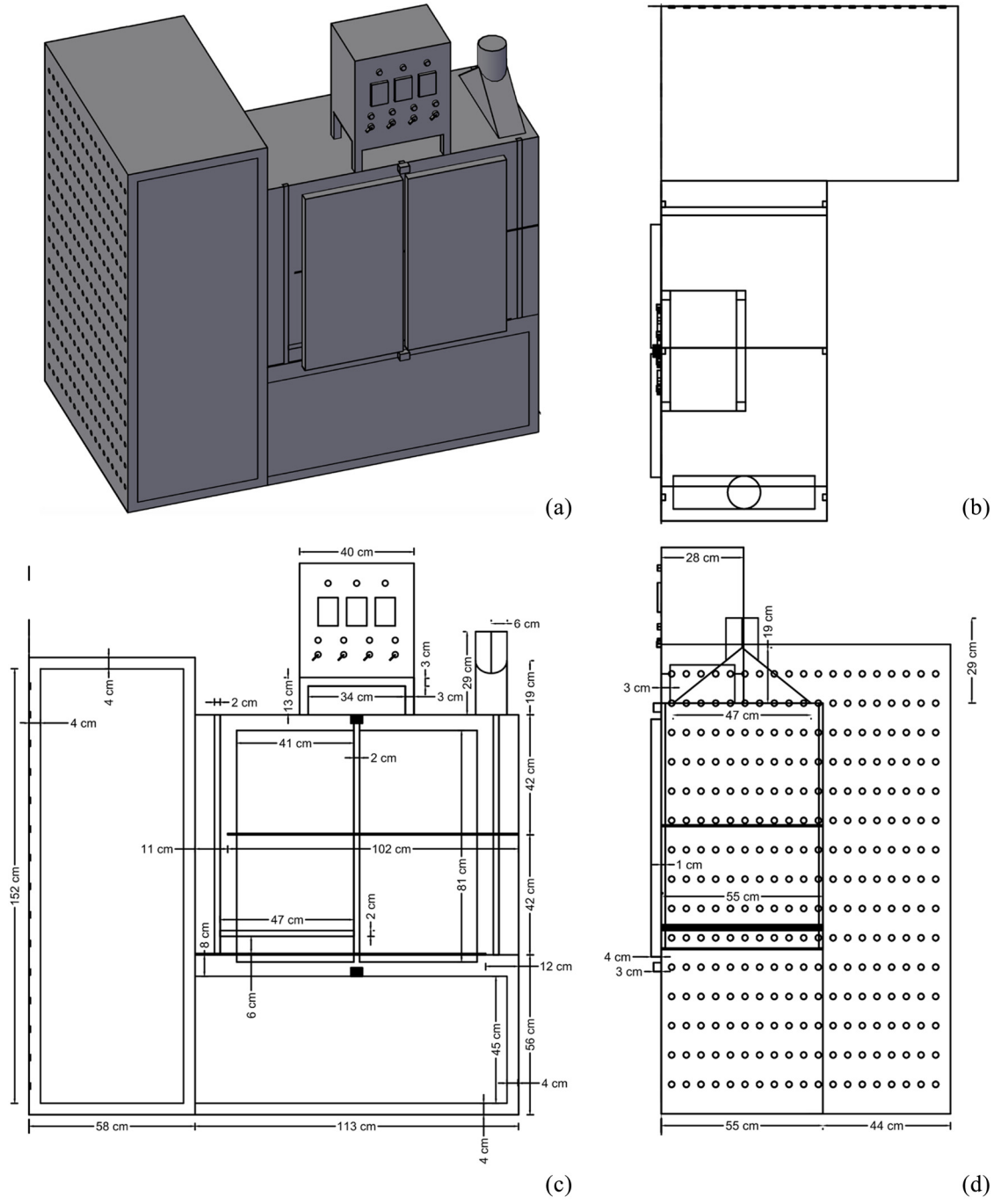

Figure 2: Design of industrial-scale heat pump drying equipment. (a) Perspective projection, (b) vertical projection, (c) equal projection, and (d) edge projection.

2.4.2 TFC

Each 5.00 ± 0.02 g soursop slices (m) were extracted with 50 mL ethanol 96° (V_1). The extract was filtered using filter towels and Whatman No.1 paper. Each 0.5 mL filtered extract (V_2) was then mixed with 0.1 mL $AlCl_3$, 4.3 mL ethanol 96°, and 0.1 mL CH_3COOK using a vortex (MX-S50Hz, DLAB Faithful, China) mixer for 30 s at 1,500 rpm (V_3). The mixture was incubated for 30 min in the dark and measured at 415 nm using UV-Vis spectroscopy.

Standard curve of Quercitrin (QE):

$$y = 176.87 \times x + 1.77. \quad (4)$$

TFC (mgQE/gDW):

$$\text{TFC} = \frac{V_1 \times C \times 100 \times V_3}{V_2 \times 1{,}000 \times m \times (100 - \text{MC}_t)}, \quad (5)$$

where C is the TFC obtained from the spectrophotometer corresponding to the cuvette volume (μg/mL).

2.4.3 ABTS and DPPH antioxidant activity

The extraction and filtration were performed as described in Section 2.4.2. Then, each 0.5 mL extract was mixed with 1.5 mL ABTS or DPPH using a vortex mixer for 30 s at 1,500 rpm (V_3). The mixture was incubated for 30 min in the dark. Samples were measured using UV-Vis spectroscopy at 734 nm for ABTS or 517 nm for DPPH. Standard curves for DPPH and ABTS antioxidant activity were based on ascorbic acid (AA) equivalent.

Standard curve of DPPH antioxidant activity:

$$y = -36.75 \times x + 28.31. \quad (6)$$

Standard curve of ABTS antioxidant activity:

$$y = -22.52 \times x + 20.16.$$

ABTS/DPPH antioxidant activity (mg AA/g DW):

$$= \frac{V_1 \times C \times 100 \times V_3}{V_2 \times 1{,}000 \times m \times (100 - \text{MC}_t)}. \quad (7)$$

2.5 Mathematical modeling and kinetic analysis of the process

2.5.1 Mathematical modeling

Drying thinly sliced fruits and vegetables is modeled by 30 mathematical models of moisture loss (Table 1) and 05 mathematical models of quality changes (Table 2), depending on drying method, conditions, dryer design, and input material.

2.5.2 Estimation of the effective moisture diffusivity

The effective moisture diffusion coefficient (D_{eff}) is essential for simulating drying processes but cannot be measured directly and must be calculated. Accurate determination of D_{eff} is crucial for realistic moisture transfer models. To determine D_{eff}, the Fick's diffusion model was applied as follows:

Table 1: 30 mathematical models of moisture loss in previous drying processes

No.	Models	Equation	Eq.	Ref.
1	Ademiluyi Modified	$MR = a \exp(-(kt)^n)$	(8)	[29]
2	Aghbashlo	$MR = \exp\{-[k_1 t/(1 + kt)]\}$	(9)	[30]
3	Balbay and Sahin	$MR = (1 - a) \exp(-kt^n) + b$	(10)	[31]
4	Binomial	$MR = a \exp(-kt) + b \exp(k_1 t)$	(11)	[32]
5	Combined Two Term and Page	$MR = a \exp(-kt^n) + (1 - a) \exp(-k_1 t)$	(12)	[33]
6	Demir et al.	$MR = a \exp(-kt)^n + b$	(13)	[34]
7	Diffusion approximation	$MR = a \exp(-kt) + (1 - a) \exp(-k_1 bt)$	(14)	[35]
8	Two-Term Exponential	$MR = a \exp(-kt) + (1 - a) \exp(-k_1 at)$	(15)	[36]
9	Hasibuan and Daud	$MR = 1 - at^n \exp(-kt^n)$	(16)	[37]
10	Henderson and Pabis	$MR = a \exp(-kt)$	(17)	[38]
11	Hii et al.	$MR = a \exp(-kt^n) + b \exp(-k_1 t^n)$	(18)	[39]
12	Logarithmic	$MR = a \exp(-kt) \pm c$	(19)	[40]
13	Logistics	$MR = b/[1 + a \exp(kt)]$	(20)	[41]
14	Midilli et al.	$MR = a \exp(-kt^n) + bt$	(21)	[42]
15	Modified Henderson and Pabis	$MR = a \exp(-kt) + b \exp(-k_1 t) + c \exp(-k_2 t)$	(22)	[43]
16	Modified Page	$MR = \exp(-kt)^n$	(23)	[42]
17	Modified Page II	$MR = \exp(-k\,(t/L^2)^n)$	(24)	[44]
18	Modified Page III	$MR = k \exp(-t/L^2)^n$	(25)	[45]
19	Newton/Lewis	$MR = \exp(-kt)$	(26)	[46]
20	Noomhorm and Verma	$MR = a \exp(-kt) + b \exp(-nt) + c$	(27)	[47]
21	Page	$MR = \exp(-kt^n)$	(28)	[48]
22	Silva et al.	$MR = \exp(-at - bt^{1/2})$	(29)	[49]
23	Simplified Fick's diffusion	$MR = a \exp(-c\,(t/L^2))$	(30)	[50]
24	Singh et al.	$MR = \exp(-kt) - akt$	(31)	[51]
25	Thompson	$t = a \ln(MR) + b \ln(MR)^2$	(32)	[52]
26	Two-term	$MR = a \exp(-kt) + b \exp(-k_1 t)$	(33)	[53]
27	Vega Lemus	$MR = (a + kt)^2$	(34)	[54]
28	Verma et al.	$MR = a \exp(-kt) + (1 - a) \exp(-k_1 t)$	(35)	[55]
29	Wang and Singh	$MR = 1 + at + bt^2$	(36)	[38]
30	Weibull	$MR = a - b \exp(-kt^n)$	(37)	[56]

Noted: a, b, c, and n are the coefficients of the models; k, k_1, and k_2 are the constants of moisture loss rate (min^{-1}); L is the thickness of the drying material (mm).

Fick's diffusion:

$$\frac{\partial M}{\partial t} = D_{\text{eff}} \frac{\partial^2 M}{\partial x^2}. \quad (43)$$

Table 2: Mathematical models describing the changes in TFC, DPPH, and ABTS antioxidant activity during previous drying processes

No.	Model name	Equation	Eq.	Ref.
1	First order (a,b,c)	$C_t = C_0 \exp(\pm kt)$	(38)	[57]
2	Fractional conversion (a)	$C_t = (C_0 - C_{eq}) \exp(\pm kt) + C_{eq}$	(39)	[58]
3	Polynomial quadratic (b)	$C = C_0 + at + bt^2$	(40)	[59]
4	Second order (a,b,c)	$1/C_t = 1/C_0 + kt$	(41)	[60]
5	Zero order (a,b)	$C_t = C_0 \pm kt$	(42)	[61]

Noted: C_0 and C_t denote the component content ratio at time $t = 0$ and $t = t$, respectively. C_{eq} is the equilibrium content. The symbol "±" indicates the formation (+) and degradation (–) of the component. Symbols (a), (b), and (c) indicate models describing DPPH, ABTS antioxidant activity, and TFC, respectively.

Crank (1975) provided solutions for moisture diffusion in other shapes.

$$\mathrm{MR} = \frac{8}{\pi^2}\sum_{n=0}^{\infty}\frac{1}{(2n+1)^2}\exp\left(-(2n+1)^2\pi^2\frac{D_{\mathrm{eff}}}{4L^2}t\right). \quad (44)$$

For extended drying periods, the equation simplifies to

$$\ln(\mathrm{MR}) = \ln\left(\frac{8}{\pi^2}\right) - \pi^2\frac{D_{\mathrm{eff}}}{4L^2}t. \quad (45)$$

Effective moisture diffusivity is determined from the slope of the ln(MR) vs time plot.

2.5.3 Estimation of E_a

The logarithm of MR vs inverse temperature gives the E_a from the slope.

Arrhenius equation:

$$D_{\mathrm{eff}} = D_0 \exp\left[-E_a\left(\frac{1}{R \times T} - \frac{1}{R \times T_{\mathrm{ref}}}\right)\right], \quad (46)$$

where E_a is the activation energy (kJ/mol), D_{eff} is the effective diffusivity, D_0 is the pre-exponential factor (m^2/s), R is the gas constant (8.314 kJ/mol), and $T = T_0$ (°C) + 273.15 is the absolute temperature (K). T_{ref} is the average absolute temperature (K). For calculating E_a for TFC, DPPH, and ABTS antioxidant activity, the slope of the $\ln(C/C_0)$ vs time plot gives rate constant (k_{Arr} = – slope). E_a is then found from the nonlinear relation between k_{Arr} and $(1/(R \times T) - 1/R \times T_{\mathrm{ref}})$ [62].

2.5.4 Determination of the coefficient of determination (R^2) and chi-square (χ^2)

Experimental data were fitted to kinetic models (Section 2.5.1) to determine the best model for MC, TFC, DPPH, and ABTS during drying. The models were evaluated using R^2, χ^2, and RMSE. The best model has the highest R^2 and lowest χ^2 and RMSE values.

$$R^2 = 1 - \frac{\sum_{i=1}^{n}(C_{\exp,i} - C_{\mathrm{pre},i})^2}{\sum_{i=1}^{n}(C_{\exp,i} - C_{\mathrm{mean}})^2}, \quad (47)$$

$$X^2 = \frac{\sum_{i=1}^{n}(C_{\exp,i} - C_{\mathrm{pre},i})^2}{N - n}, \quad (48)$$

$$\mathrm{RMSE} = \left(\frac{\sum_{i=1}^{N}(C_{\exp,i} - C_{\mathrm{pre},i})^2}{N - n}\right)^{\frac{1}{2}}, \quad (49)$$

where N and n: total experimental and predicted data points. $C_{\exp,i}$: experimental value at i, and $C_{\mathrm{pre},i}$: predicted value, C_{mean}: mean experimental value [63].

2.6 Statistical and data analysis

Data were analyzed with Microsoft Excel (Redmond, WA, USA) and one-way ANOVA was conducted using IBM® SPSS® Statistics version 25, with significance set at a 95% confidence interval. Tukey HSD[a,b] tested the significance of differences in the study. Additionally, Origin Pro 9.0 software, version 90E (OriginLab, Roundhouse Plaza Northampton, USA), was utilized for further analysis [28].

3 Results and discussion

3.1 Drying curve and DR

The initial MC of soursop slices dried at 20–50°C averaged 77.03 ± 1.15 kg water/kg solid for slices about 1.3 mm thick. Changes in MC over time were expressed as the MR (Figure 3).

Figure 3 shows that MC decreases with increased drying time and faster DRs at higher temperatures ($p < 0.05$). The time to reach stable MC (MR < 0.02 kg water/kg solid) at 20, 30, 40, and 50°C were 1,080, 750, 465, and

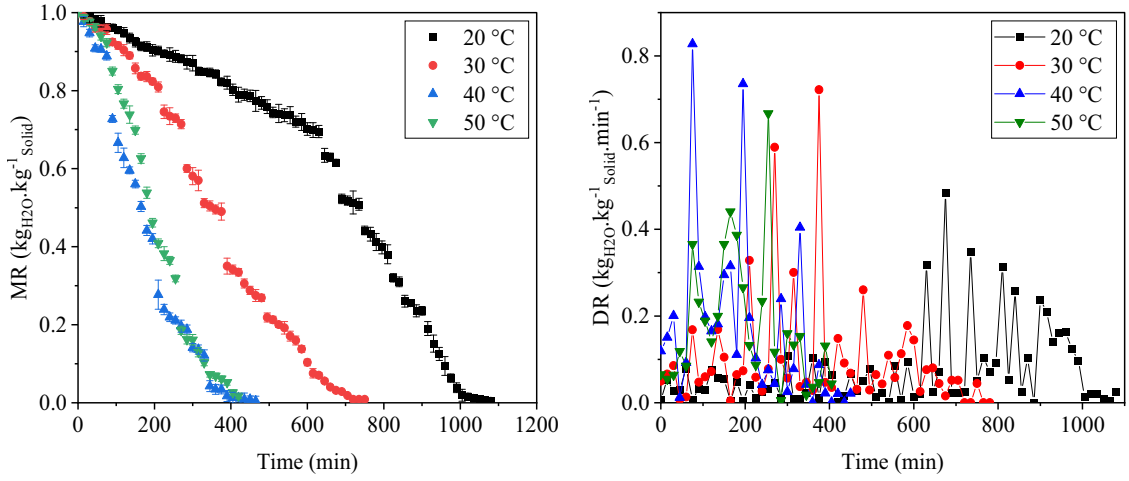

Figure 3: MC and DR of soursop slices during industrial-scale heat pump drying. The results are repeated with n = 3.

420 min, respectively. This indicates significant effects of both temperature and drying time on soursop slices' MC (p < 0.05). Similar findings were reported for turmeric slices dried with hot air and infrared support at 50–70°C [64]. Temperature variation is inversely proportional to drying time. Increasing the temperature accelerates water evaporation, leading to shorter drying time. This is consistent with the findings from most of the previous drying processes. For example, the heat pump drying time for 10 mm thick mango slices decreased from 1,400 to 700 min as the temperature increased from 20 to 50°C [25]. Increasing the hot air drying temperature for 5 mm apple slices from 40 to 60°C reduced drying time from 400 to 240 min [65]. Differences in drying techniques, equipment, and conditions affect moisture diffusion and drying time. At 20°C, drying occurs in two stages: a slow diffusion stage removing 30% of moisture in the first 630 min, followed by a rapid increase to 98% by 1,005 min, and then stabilization up to 1,080 min. Initially, moisture loss is slow due to the humidity difference. In the next stage, after 30% moisture loss, larger cell pores and faster water movement accelerate drying. Moisture reduction slows significantly when the humidity difference decreases [30]. At higher temperatures, continuous moisture reduction makes constant DR stages hard to identify. This shows that heat pump drying and equipment design allow balanced moisture movement and diffusion. Similar results were found for thin-layer liquorice root drying at 40–55°C [31]. The DR at 40°C is faster than at 50°C in industrial heat pump drying. Moderate heat and low humidity at 40°C increase moisture loss, while higher temperatures (50°C) cause cell shrinkage and blocked pores, slowing the DR [41]. A report on drying apple slices at 40–50°C showed that reaching MR < 0.02 kg water/kg solid took approximately 700–400 min [66]. A previous report on drying lotus pollen at 40 and 50°C found no significant difference in drying time [67].

On the other hand, the DR changes significantly and fluctuates strongly over time. In the initial stage of the drying process, moisture on the surface of the material is quickly lost, leading to a high DR. As the surface moisture becomes depleted, the DR decreases. As drying continues, moisture from within the material moves to the surface. This movement causes temporary decreases in the DR, resulting in the formation of sharp peaks. Additionally, each drying temperature affects the material differently. At a low temperature (20°C), the drying process is slower and the DR is more stable but lower overall. The findings suggest that the moisture loss rate appears to be fastest when the MC in the sample fluctuates between 0.5 and 0.6 kg water/kg solid, corresponding to a 40–50% reduction in MC compared to the initial moisture level. A previous report also showed similar results regarding the variation and temporary decrease in DR during the drying process of tomato slices using convective hot air drying [68] and heat pump drying of Tu Quy mango slices [25].

3.2 Mathematical models of moisture loss

A total of 30 mathematical models were developed to describe previous drying processes and predict moisture diffusion in drying soursop slices. Among these, 24 models were considered highly suitable (R^2 > 0.7).

Table 3: Statistical results and regression coefficients of models describing moisture loss

No.	Models	Para.	20°C	30°C	40°C	50°C
1	Ademiluyi Modified	χ^2	0.00161	0.00052	0.00087	0.00044
		RMSE	0.04014	0.02278	0.0296	0.02100
		R^2	0.98485	0.99590	0.99323	0.99681
2	Aghbashlo	χ^2	0.00043	0.00145	0.00154	0.00184
		RMSE	0.02084	0.03808	0.03921	0.04289
		R^2	0.99586	0.98829	0.98770	0.98620
3	Balbay and Sahin	χ^2	0.00100	0.00048	0.00087	0.00046
		RMSE	0.03164	0.02208	0.02957	0.02141
		R^2	0.99073	0.99622	0.99347	0.99682
4	Combined Two Term and Page	χ^2	0.18795	0.00131	0.00094	0.00047
		RMSE	0.43353	0.03622	0.03065	0.02172
		R^2	−0.71631	0.99006	0.99324	0.99686
5	Diffusion approximation	χ^2	0.01163	0.00266	0.0013	0.00234
		RMSE	0.10787	0.05160	0.03611	0.04838
		R^2	0.89063	0.97895	0.98992	0.98309
6	Two-Term Exponential	χ^2	0.02751	0.01682	0.00131	0.01844
		RMSE	0.16586	0.12967	0.03616	0.13578
		R^2	0.74140	0.86702	0.98989	0.86681
7	Hasibuan and Daud	χ^2	0.26070	0.41935	0.00639	0.00526
		RMSE	0.51060	0.64757	0.07996	0.07256
		R^2	−1.45080	−2.31620	0.94717	0.96197
8	Henderson and Pabis	χ^2	0.02149	0.01075	0.00611	0.01144
		RMSE	0.14659	0.10367	0.07817	0.10696
		R^2	0.79510	0.91324	0.95113	0.91416
9	Hii et al.	χ^2	0.00540	0.00056	0.00094	0.00048
		RMSE	0.07347	0.02335	0.03068	0.02186
		R^2	0.95070	0.99587	0.99222	0.99681
10	Logistics	χ^2	0.10423	0.40053	0.00094	0.00044
		RMSE	0.32285	0.63287	0.03063	0.02095
		R^2	0.02015	−2.62110	0.99275	0.99683
11	Modified Henderson and Pabis	χ^2	0.02277	0.01170	0.00705	0.01343
		RMSE	0.15090	0.10818	0.08397	0.11589
		R^2	0.79510	0.91324	0.95113	0.91416
12	Modified Page	χ^2	0.02712	0.01647	0.00964	0.01775
		RMSE	0.16469	0.12834	0.09817	0.13324
		R^2	0.74140	0.86702	0.92293	0.86681
13	Modified Page II	χ^2	0.00420	0.00061	0.00085	0.00044
		RMSE	0.06479	0.02471	0.02917	0.02099
		R^2	0.95998	0.99507	0.99319	0.99669
14	Newton/Lewis	χ^2	0.02674	0.01614	0.00933	0.00933
		RMSE	0.16354	0.12705	0.09657	0.09657
		R^2	0.74140	0.86702	0.92293	0.92293
15	Page	χ^2	0.00445	0.00061	0.00085	0.00044
		RMSE	0.06668	0.02477	0.02918	0.02099
		R^2	0.95761	0.99505	0.99319	0.99669
16	Silva et al.	χ^2	0.48005	0.01647	0.00964	0.01775
		RMSE	0.69286	0.12834	0.09817	0.13324
		R^2	−3.57720	0.86702	0.92293	0.86681
17	Simplified Fick's diffusion	χ^2	0.02149	0.01075	0.00611	0.01144
		RMSE	0.14659	0.10367	0.07817	0.10696
		R^2	0.79510	0.91324	0.95113	0.91416
18	Singh et al.	χ^2	0.01332	0.00340	0.00243	0.00477
		RMSE	0.11543	0.05830	0.04934	0.06904
		R^2	0.87296	0.97256	0.98053	0.96424
19	Thompson	χ^2	0.25484	0.05524	0.04100	0.01312
		RMSE	0.50481	0.23503	0.20248	0.11452

(Continued)

Table 3: *Continued*

No.	Models	Para.	20°C	30°C	40°C	50°C
		R^2	0.85288	0.97115	0.98583	0.99125
20	Two-term	χ^2	0.02211	0.01120	0.00655	0.01236
		RMSE	0.14870	0.10585	0.08092	0.11116
		R^2	0.79510	0.91324	0.95113	0.91416
21	Vega Lemus	χ^2	0.01504	0.00415	0.00171	0.00449
		RMSE	0.12264	0.06443	0.04139	0.06700
		R^2	0.85658	0.96649	0.98630	0.96632
22	Verma et al.	χ^2	0.02127	0.00992	0.00487	0.00961
		RMSE	0.14584	0.09962	0.06979	0.09804
		R^2	0.80003	0.92152	0.96234	0.93057
23	Wang and Singh	χ^2	0.00128	0.00333	0.00285	0.00476
		RMSE	0.03573	0.05770	0.05340	0.06901
		R^2	0.98783	0.97312	0.97719	0.96428
24	Weibull	χ^2	0.00361	0.00061	0.00085	0.00044
		RMSE	0.06012	0.02463	0.02917	0.02099
		R^2	0.96554	0.95510	0.99319	0.99670

Noted: The Binomial, Demir, Midilli, Modified Page III, Noomhorm and Verma, and Weibull models are unsuitable for drying soursop slices ($R^2 < 0.2$).

Table 4: Models, statistical parameters, and half-life of MC

No.	Models	Temp. (°C)	R^2	Constants and coefficients	T50 (min)
1	Aghbashlo	20	0.99586	$k = -0.91 \times 10^{-3}$ $k_1 = 0.31 \times 10^{-3}$	737.10
2	Balbay and Sahin	30	0.99622	$k = 0.28 \times 10^{-5}$ $a = -0.01$ $b = -0.03$ $n = 2.11$	347.83
3	Balbay and Sahin	40	0.99347	$k = 14.02 \times 10^{-4}$ $a = -0.02$ $b = -0.02$ $n = 1.67$	160.19
4	Logistics	50	0.99683	$k = 15.43 \times 10^{-3}$ $a = 0.06$ $b = 1.06$	189.68

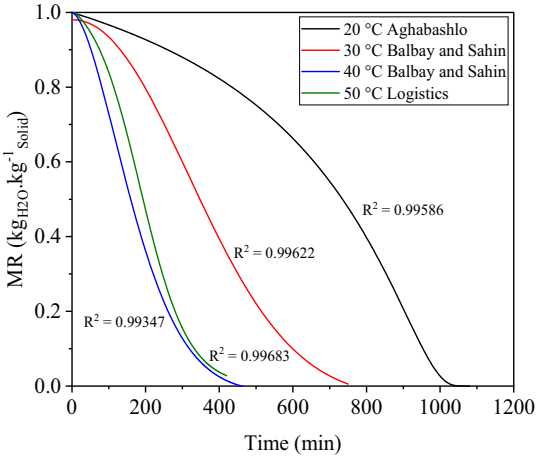

Figure 4: Four mathematical models describing the moisture loss mechanism in heat pump drying of soursop slices at different temperatures.

$$MR20 = \exp[(-0.31 \times 10^{-3}t)/(1 - 0.91 \times 10^{-3}t)], \quad (50)$$

$$MR30 = 1.01 \ \exp(-0.280 \times 10^{-5}t^{2.11}) - 0.03, \quad (51)$$

$$MR40 = 1.02 \ \exp(-14.02 \times 10^{-5}t^{1.67}) - 0.02, \quad (52)$$

$$MR50 = 1.06/[1 + 0.06 \ \exp(15.43 \times 10^{-3}t)]. \quad (53)$$

Table 3 shows the mathematical models predicting the drying curves of soursop slices, with most fitting the data well ($R^2 > 0.8$). The models selected for heat pump drying at 20–50°C are Aghbashlo, Balbay and Sahin, and Logistics (Table 4 and Figure 4). At 20°C, moisture loss occurs via two mechanisms, while at higher temperatures, it follows a single mechanism. Figure 4 illustrates predicted drying curves for industrial-scale heat pump drying. The half-moisture reduction times at 20, 30, 40, and 50°C are 737.10, 347.83, 160.19, and 189.68 min, respectively. A similar study on drying licorice root at 40°C found the Balbay and Sahin model to be highly suitable ($R^2 > 0.99$) [31].

3.3 Estimating the E_a of MC

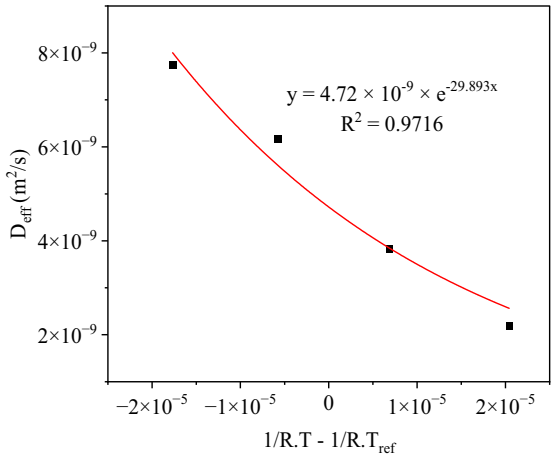

Figure 5: The relationship between D_{eff} and $\frac{1}{R \times T} - \frac{1}{R \times T_{ref}}$ at different drying temperatures.

$$y_{20} = -0.0032x + 0.8324 \quad R^2 = 0.6056, \tag{54}$$

$$y_{30} = -0.0056x + 0.8087 \quad R^2 = 0.8356, \tag{55}$$

$$y_{40} = -0.0090x + 0.6498 \quad R^2 = 0.9075, \tag{56}$$

$$y_{50} = -0.0113x + 0.8287 \quad R^2 = 0.9094. \tag{57}$$

E_a was determined using the Arrhenius equation based on the plot of ln(MR) and $(1/R\,T - 1/R\,T_{ref})$ for the four drying temperatures 20–50°C (Figure 5). Diffusion coefficients at 20, 30, 40, and 50°C were 2.2×10^{-9}, 3.8×10^{-9}, 6.2×10^{-9}, and 7.7×10^{-9} (m^2/s), respectively, indicating that a 10°C increase in drying temperature increases diffusion efficiency by 1.5–2 times. The calculated E_a for moisture removal from soursop slices in industrial-scale heat pump drying was E_a = 29.89 kJ/mol. This result aligns with most reported drying processes for vegetables and fruits, with about 90% of activation energies ranging from 14.42 to 43.26 kJ/mol [69]. Similarly, avocado slice drying reported a comparable E_a (E_a = 32.06 kJ/mol) [70].

3.4 Degradation curves of TFC

Flavonoids are a major group of polyphenols responsible for significant antioxidant activity. The initial TFC was 4.69 ± 0.11 mgQE/gDW. The degradation of TFC over time is shown as the ratio of content at time t to t = 0 (Figure 6).

TFC is significantly affected by the drying process due to its sensitivity to temperature and oxygen ($p < 0.05$) [71,72]. At low temperatures (20°C), the decline in TFC is

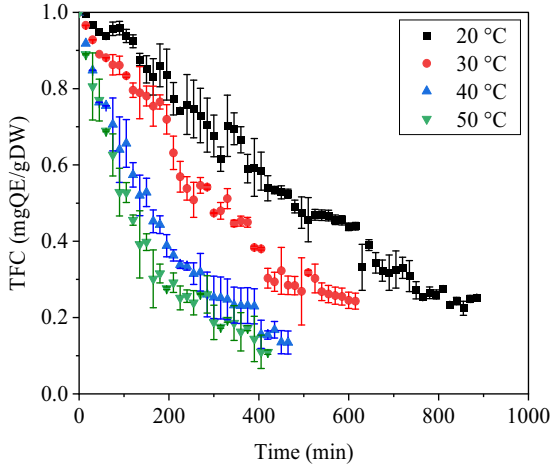

Figure 6: TFC of soursop slices during industrial-scale heat pump drying. The results are repeated with n = 3.

mainly due to the presence of oxygen in the drying agent, rather than the temperature itself [73]. Oxidation and degradation intensify as drying temperature increases to 30, 40, and 50°C. At 30 and 40°C, high moisture and heat promote reactions with oxygen, causing significant TFC loss. The difference between 40 and 50°C is smaller due to cell shrinkage limiting heat and oxygen penetration, which protects bioactive compounds. However, high temperatures still significantly degrade flavonoids. Similar findings were reported for pomegranate arils, where increasing drying temperatures from 55 to 75°C decreased flavonoids,

Table 5: Statistical results and regression coefficients of models describing the degradation of TFC

No.	Models	Para.	20°C	30°C	40°C	50°C
1	First order	χ^2	0.00222	0.00168	0.00059	0.00156
		RMSE	0.04717	0.04097	0.02433	0.03954
		R^2	0.96339	0.97186	0.99030	0.97480
2	Second order	χ^2	0.04064	0.00563	0.00325	0.00863
		RMSE	0.20160	0.07503	0.05701	0.09290
		R^2	0.33110	0.90560	0.94680	0.86110

Table 6: Models, statistical parameters, and half-life of TFC

No.	Models	Temp. (°C)	R^2	Constants and coefficients	T50 (min)
1	First order	20	0.96339	$k = 14.5 \times 10^{-4}$	478.03
2	First order	30	0.97186	$k = 23.2 \times 10^{-4}$	298.77
3	First order	40	0.99030	$k = 44.8 \times 10^{-4}$	154.72
4	First order	50	0.97480	$k = 58.9 \times 10^{-4}$	117.68

polyphenols, and anthocyanins, with minimal differences between 65 and 75°C [74]. A drying study on button mushrooms showed that at 70°C, significant cell shrinkage occurs, and at 65°C, the TFC degradation curves are nearly identical [75]. This suggests that at temperatures causing strong cell shrinkage, pore closure occurs. Each material undergoes shrinkage at a specific temperature during the drying process. Soursop slices were found to experience significant shrinkage at temperatures above 40°C.

3.5 Mathematical models of the degradation of TFC

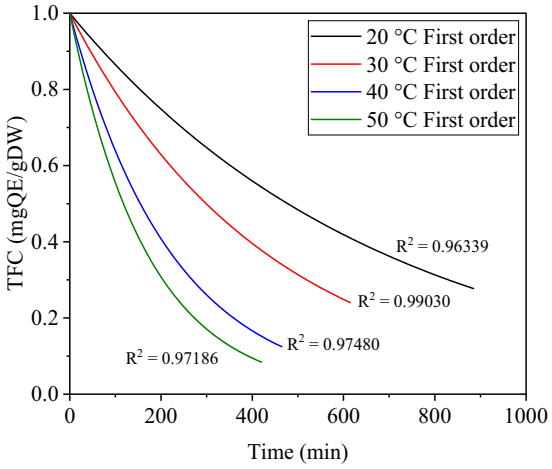

Figure 7: Four mathematical models describing the degradation TFC mechanism in heat pump drying of soursop slices at different temperatures.

$$C_{t20} = C_0 \exp(-14.5 \times 10^{-4} t), \quad (58)$$

$$C_{t30} = C_0 \exp(-23.2 \times 10^{-4} t), \quad (59)$$

$$C_{t40} = C_0 \exp(-44.8 \times 10^{-4} t), \quad (60)$$

$$C_{t50} = C_0 \exp(-58.9 \times 10^{-4} t). \quad (61)$$

The degradation of flavonoid compounds in soursop slices was analyzed using both First-order and Second-order mathematical models at four drying temperatures (20–50°C). The results showed that the First-order model is suitable for describing TFC degradation, with $R^2 > 0.96$, $\chi^2 < 0.0022$, and RMSE < 0.047 (Tables 5 and 6). The predicted data and degradation models are illustrated in Figure 7. The rate constants k at 20, 30, 40, and 50°C were 14.5×10^{-4}, 23.2×10^{-4}, 44.8×10^{-4}, and 58.9×10^{-4}, respectively. This indicates an increase in DR by 1.3–1.9 times for every 10°C rise from 20 to 40°C. However, from 40 to 50°C, the rate only increased 1.3 times. This is consistent with the findings on drying pomegranate arils [74] and button mushrooms [75], where DRs increased from 55 to 65°C but less so from 65 to 75°C. Based on the chosen models, the half-life times for TFC degradation were 478.03, 298.77, 154.72, and 117.68 min at 20, 30, 40, and 50°C, respectively.

3.6 Estimating the E_a of TFC

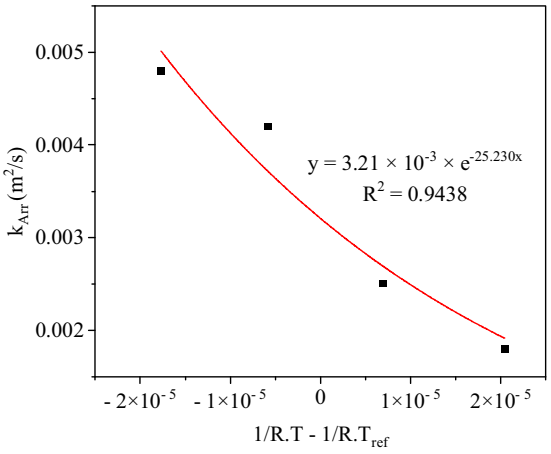

Figure 8: Relationship between k_{Arr} of total flavonoids content and $\frac{1}{R \times T} - \frac{1}{R \times T_{ref}}$ at different drying temperatures.

$$y_{20} = -0.0018x + 0.1233 \quad R^2 = 0.9757, \quad (62)$$

$$y_{30} = -0.0025x + 0.0532 \quad R^2 = 0.9730, \quad (63)$$

$$y_{40} = -0.0042x - 0.0580 \quad R^2 = 0.9847, \quad (64)$$

$$y_{50} = -0.0048x - 0.1525 \quad R^2 = 0.9648. \quad (65)$$

E_a is the minimum energy needed for reactions to occur, with lower Ea indicating easier degradation with slight temperature increases [75]. The E_a for flavonoid degradation is 25.23 kJ/mol (Figure 8), similar to button mushrooms at 25.38 kJ/mol [75]. This suggests flavonoids degrade more easily by heat than by moisture removal or antioxidant activities (DPPH and ABTS). Flavonoids, after degradation, still exhibit antioxidant properties. This is due to the decrease in flavonoid content but an increase in antioxidant activity from new compounds formed. For example, quercetin can convert into quercetin-3-glucuronide and quercetin-3-sulfate under high heat during drying [76]. This transformation occurs due to the breakdown of the original molecular structure and reformation into new compounds under

heat and oxygen. Additionally, flavonoids can transform into other antioxidant compounds, losing their flavonoid identity. Catechin, for instance, can convert into catechol, a simpler phenolic, but still retains antioxidant capabilities. Other flavonoids like anthocyanin, flavanones, quercetin, kaempferol, isoflavonoid, and hesperidin degrade into compounds such as caffeic acid, gallic acid, ferulic acid, anthocyanidin, chalcone, stilbene, isoflavone, and hesperetin. These compounds have antioxidant properties but are not classified as flavonoids [77,78].

3.7 Decline curves of antioxidant activities

The antioxidant activity of soursop slices was tested using DPPH and ABTS radicals. Initial DPPH and ABTS antioxidant activities were 4.42 ± 0.06 mg AA/g DW and 3.84 ± 0.02 mg AA/g DW, respectively. Changes in antioxidant activity over time are shown as the ratio of content at time t to t = 0 (Figure 9).

The antioxidant activity results based on DPPH and ABTS (Figure 9) revealed an inverse correlation between time, temperature, and antioxidant activity. Statistical analysis showed significant differences in antioxidant activity with drying times and temperatures from 20 to 50°C (p < 0.05). Measurements continued until the MC reached a very slow reduction phase. The drying times for DPPH and ABTS antioxidant activities to stabilize at 20, 30, 40, and 50°C were 885, 615, 465, and 420 min, respectively. Drying generally decreases quality regardless of conditions. For tea production, maintaining antioxidant components is crucial. The study showed that increasing drying temperature and time significantly reduced antioxidant activity. Higher temperatures caused faster declines, likely due to the sensitivity of bioactive compounds like polyphenols, vitamin C, and flavonoids to heat, which are key antioxidants in the material [71,72]. After the first hour of drying at 20°C, DPPH antioxidant activity decreased by 8%, while ABTS antioxidant activity dropped by 16%. About 90% of DPPH and ABTS antioxidant activities were reduced after 795 and 870 min, respectively. Initially, DPPH antioxidant activity declines faster but slows compared to ABTS later. The decomposition rate at 20°C is mainly due to oxygen exposure [73]. At 30, 40, and 50°C, DPPH and ABTS antioxidant activities decrease linearly and slow down near the end of the drying process. This is likely because low water content at the end reduces chemical reactions. As water is removed, antioxidants may become more concentrated, enhancing internal interactions and slowing degradation. Previous studies also show a gradual decline in bioactive compounds and antioxidant activity towards the end of drying at 55–75°C [74]. Another report indicates a positive correlation between the decline of polyphenol compounds and ABTS antioxidant activity [79].

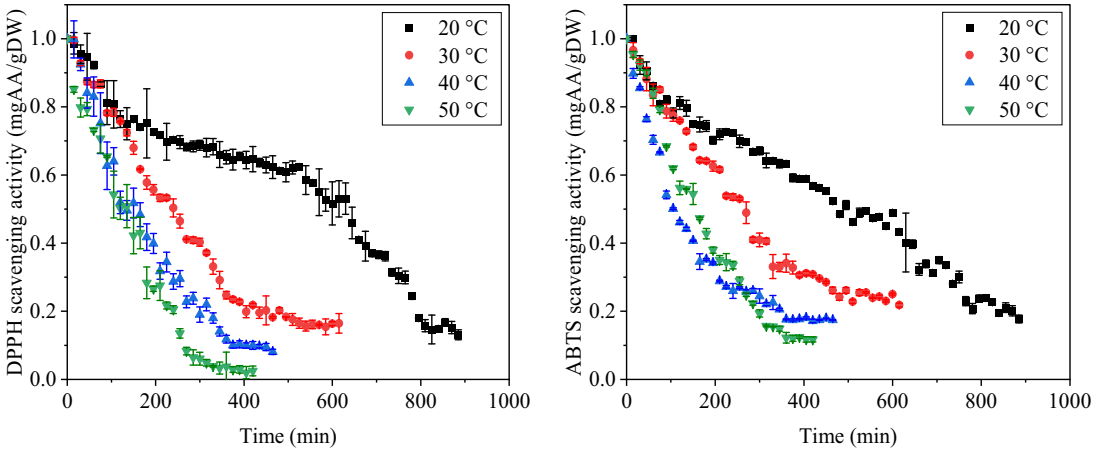

Figure 9: DPPH and ABTS antioxidant activities of soursop slices during industrial-scale heat pump drying. The results are repeated with n = 3.

Table 7: Statistical results and regression coefficients of models describing the degradation of DPPH and ABTS antioxidant activity

Indicators	No.	Models	Para.	20°C	30°C	40°C	50°C
DPPH antioxidant activity	1	First order	χ^2	0.00694	0.00168	0.01480	0.00385
			RMSE	0.08328	0.04099	0.03845	0.06202
			R^2	0.86749	0.97825	0.98275	0.95974
	2	Fractional conversion	χ^2	0.00801	0.00458	0.00282	0.00462
			RMSE	0.08949	0.06764	0.05306	0.06795
			R^2	0.84699	0.94077	0.96714	0.95166
	3	Second order	χ^2	0.04595	0.00854	0.01155	0.02828
			RMSE	0.21437	0.09239	0.10748	0.16815
			R^2	0.12208	0.88949	0.86520	0.70463
	4	Zero order	χ^2	0.00444	0.00908	0.01268	0.01558
			RMSE	0.06666	0.09529	0.11261	0.12481
			R^2	0.91512	0.88244	0.85203	0.83693
ABTS antioxidant activity	1	First order	χ^2	0.00212	0.00092	0.00241	0.00199
			RMSE	0.04608	0.03040	0.04912	0.04463
			R^2	0.95721	0.98468	0.95787	0.97673
	2	Polynomial Quadratic	χ^2	0.00162	0.00056	0.00190	0.00071
			RMSE	0.04028	0.02376	0.04355	0.02661
			R^2	0.96787	0.99087	0.96795	0.99202
	3	Second order	χ^2	0.03170	0.00408	0.00620	0.01114
			RMSE	0.17804	0.06391	0.07872	0.10554
			R^2	0.36131	0.93230	0.89183	0.86987
	4	Zero order	χ^2	0.00256	0.00826	0.02970	0.00745
			RMSE	0.05060	0.09089	0.17234	0.08630
			R^2	0.94841	0.86311	0.48146	0.91297

3.8 Mathematical models of the decline in antioxidant activities

$$C_{t20\mathrm{DPPH}} = C_0 - 0.00093t, \quad (66)$$

$$C_{t30\mathrm{DPPH}} = C_0 \ \exp(-0.00321t), \quad (67)$$

$$C_{t40\mathrm{DPPH}} = C_0 \ \exp(-0.00501t), \quad (68)$$

$$C_{t50\mathrm{DPPH}} = C_0 \ \exp(-0.00658t), \quad (69)$$

$$C_{t20\mathrm{ABTS}} = C_0 - 0.00121t + 3.48 \times 10^{-7}t^2, \quad (70)$$

$$C_{t30\mathrm{ABTS}} = C_0 - 0.00250t + 2.02 \times 10^{-6}t^2, \quad (71)$$

$$C_{t40\mathrm{ABTS}} = C_0 - 0.00472t + 6.64 \times 10^{-6}t^2, \quad (72)$$

$$C_{t50\mathrm{ABTS}} = C_0 - 0.00384t + 4.01 \times 10^{-6}t^2. \quad (73)$$

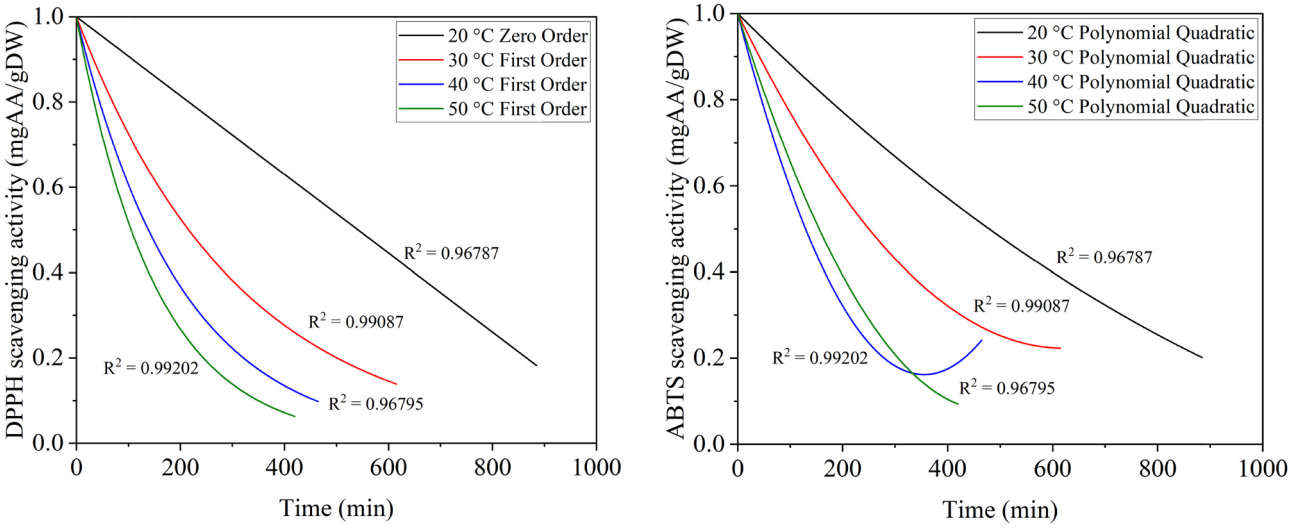

Figure 10: Four mathematical models describing the degradation DPPH and ABTS antioxidant activity mechanism in heat pump drying of soursop slices at different temperatures.

Table 8: Models, statistical parameters, and half-life of DPPH and ABTS antioxidant activity

Indicators	No.	Models	Temp. (°C)	R^2	Constants and coefficients	T50 (min)
DPPH antioxidant activity	1	Zero order	20	0.91512	k = 0.00093	537.63
	2	First order	30	0.97825	k = 0.00321	215.93
	3	First order	40	0.98275	k = 0.00501	138.35
	4	First order	50	0.95974	k = 0.00658	105.34
ABTS antioxidant activity	1	Polynomial Quadratic	20	0.96787	a = −0.00121 b = 3.48 × 10^{-7}	479.29
	2	Polynomial Quadratic	30	0.99087	a = −0.00250 b = 2.02 × 10^{-6}	250.84
	3	Polynomial Quadratic	40	0.96795	a = −0.00472 b = 6.64 × 10^{-6}	129.54
	4	Polynomial Quadratic	50	0.99202	a = −0.00384 b = 4.01 × 10^{-6}	155.25

A total of four mathematical models were developed to describe the degradation of DPPH and ABTS antioxidant activities during drying. The fitting results showed a high degree of accuracy with R^2 > 0.7 (Table 7). However, two models – zero order (20°C) and first order (30, 40, and 50°C) – were found to be the best for describing the decline in DPPH antioxidant activity at respective temperatures (R^2 > 0.91). Similarly, the Polynomial Quadratic model was best for describing the decline in ABTS antioxidant activity at all four temperatures (Figure 10). High R^2, low RMSE and χ^2 values were used to determine the best models. The rate constant k showed that degradation rate increases from 0.00093 to 0.00658 (m^2/s) as drying temperature rises to 50°C, indicating higher temperatures accelerate the degradation of bioactive components, leading to reduced antioxidant activity in soursop slices during industrial heat pump drying. Based on these models, the half-life of DPPH antioxidant activity at 20°C was 537.63 min, decreasing to 105.34 min at 50°C. For ABTS antioxidant activity, the half-life decreased from 479.29 min at 20°C to 155.25 min at 50°C. These results are consistent with previous reports on the DPPH antioxidant activity of pomegranate seeds [74], cabbage [14], and tomatoes [80] during drying at temperatures from 40 to 75°C, all following the first-order model. Similarly, the Polynomial Quadratic model was also chosen to describe the decline in antioxidant activity in pear slices, with R^2 > 0.9 (Table 8) [61].

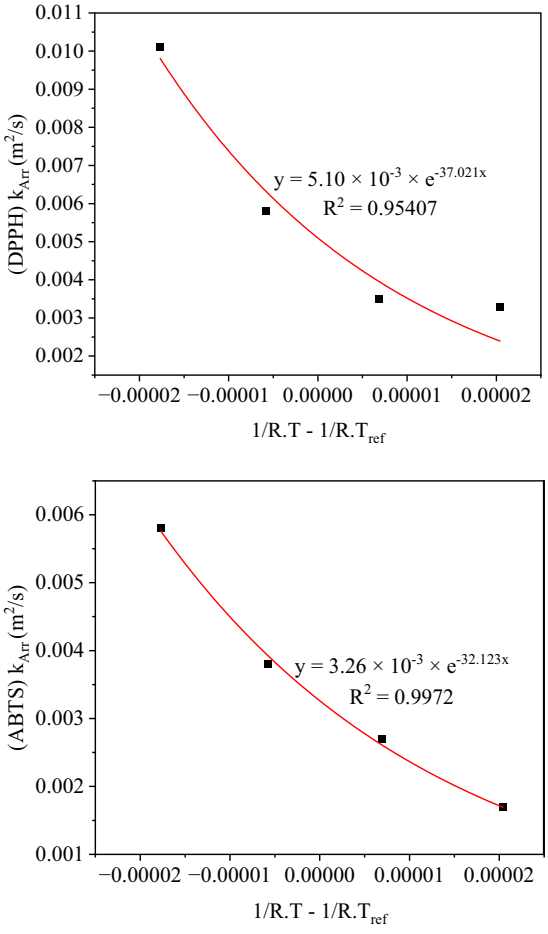

Figure 11: Relationship between k_{Arr} of DPPH and ABTS antioxidant activities and $\frac{1}{R\times T} - \frac{1}{R\times T_{ref}}$ at different drying temperatures.

3.9 Estimating the E_a of antioxidant activities

$$y_{20DPPH} = -0.0033x + 0.6336 \quad R^2 = 0.6827, \tag{74}$$

$$y_{30DPPH} = -0.0035x + 0.0604 \quad R^2 = 0.9720, \tag{75}$$

$$y_{40DPPH} = -0.0058x + 0.1187 \quad R^2 = 0.9853, \tag{76}$$

$$y_{50DPPH} = -0.0101x + 0.3928 \quad R^2 = 0.9588, \tag{77}$$

$$y_{20ABTS} = -0.0017x + 0.0690 \quad R^2 = 0.9357, \tag{78}$$

$$y_{30ABTS} = -0.0027x - 0.0169 \quad R^2 = 0.9684, \tag{79}$$

$$y_{40ABTS} = -0.0038x - 0.2346 \quad R^2 = 0.9391, \tag{80}$$

$$y_{50ABTS} = -0.0058x + 0.1400 \quad R^2 = 0.9866. \tag{81}$$

The rate constants k_{Arr} = – Slope were determined from the slope of the experimental data curve. E_a was calculated using the Arrhenius equation based on the plot of k_{Arr} vs ($1/R\,T - 1/R\,T_{ref}$) at drying temperatures of 20–50 °C (Figure 11). The calculated rate constants k_{Arr} for DPPH antioxidant activity at 20, 30, 40, and 50°C were 0.0033, 0.0035, 0.0058, and 0.0101 (m^2/s), respectively This shows that for every 10°C increase in drying temperature, k_{Arr} increases 1.06–1.74 times, with larger differences at higher temperatures. The E_a for the decline in DPPH antioxidant activity in soursop slices during industrial heat pump drying was found to be E_a = 37.02 kJ/mol. Similarly, the rate constants k_{Arr} for ABTS antioxidant activity at 20, 30, 40, and 50°C were 0.0017, 0.0027, 0.0038, and 0.0058 (m^2/s), respectively. This indicates that ABTS antioxidant activity declines more slowly than DPPH at the same temperatures, suggesting that bioactive components (such as polyphenols, flavonoids, or vitamin C) that tend to accept electrons instead of H+ were significantly degraded during drying, reducing DPPH antioxidant activity efficiency. Additionally, the k_{Arr} values suggest that with every 10°C increase, the decline in antioxidant activity increased by 1.4 to 1.5 times. The E_a for the decline in ABTS antioxidant activity in soursop slices during industrial heat pump drying was found to be E_a = 32.12 kJ/mol.

3.10 Correlation among MC, TFC, and antioxidant activities at different drying temperatures

In-depth analysis of the correlation between MC and bioactive components (TFC, DPPH, and ABTS) at various heat pump drying temperatures (20–50°C) shows strong relationships, allowing qualitative inferences about one indicator based on known values of others. The results shown in Figure 12 reveal that most correlations between MC and bioactive components at the four investigated temperatures are high to very high ($R^2 \geq 0.81$). Notably, the correlation between moisture diffusion at 30°C and the decline in ABTS antioxidant activity at 40°C is R^2 = 0.81. Similarly, the correlation between moisture diffusion at 30°C and TFC degradation at 50°C is R^2 = 0.83. However, a very close relationship was found between TFC degradation at 50°C and ABTS antioxidant activity decline at 40°C (R^2 ~ 1) [81]. The correlation between ABTS and DPPH antioxidant activity at each temperature from 20 to 50°C is also very high (R^2 > 0.97) [81]. These values enable relatively accurate predictions when one of these indicators is known. Additionally, DPPH antioxidant activity can be qualitatively inferred based on MC at each corresponding temperature due to the very high positive correlation (R^2 > 0.98). Similarly, TFC, DPPH, and ABTS can qualitatively infer each other based on a correlation of R^2 > 0.97 [81]. In the heat pump drying of soursop slices on an industrial scale, a close relationship between DPPH and ABTS decline was also noted in the drying of Hibiscus cannabinus leaves (R^2 = 0.906). The close relationship between TFC and ABTS and DPPH antioxidant activity has also been reported [81], showing similar results with correlations ranging from 0.8547 to 0.9503 [82].

4 Conclusion

This study successfully developed mathematical models to describe the drying process of soursop slices using industrial-

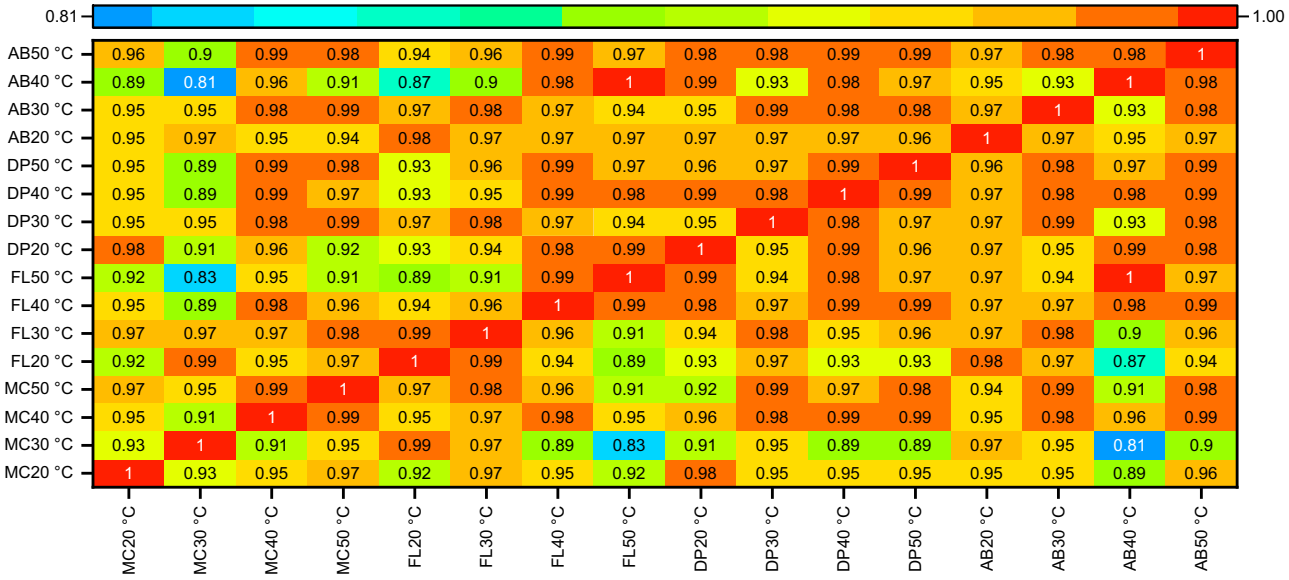

Figure 12: Correlation among the variation in MC, TFC, and antioxidant activities at drying temperatures from 20 to 50°C.

scale heat pump drying. The models accurately predicted the changes in MC (Aghbashlo, Balbay and Sahin, and Logistics), TFC (First order), and antioxidant activities (Zero order, First order, and Polynomial Quadratic) at varying temperatures (20–50°C). It was found that higher drying temperatures led to faster moisture loss and also accelerated the degradation of flavonoids and the decline in antioxidant activities of the dried samples. Additionally, the activation energies for MC, TFC, DPPH antioxidant activity, and ABTS antioxidant activity during heat pump drying were calculated as 29.89, 25.23, 37.02, and 32.12 kJ/mol, respectively. Moreover, a strong correlation between TFC and both DPPH and ABTS antioxidant activities under the same drying conditions was revealed, with $R^2 > 0.93$. The study highlights the efficiency of heat pump drying in preserving the quality of soursop tea and provides a basis for optimizing drying processes to enhance product quality and economic efficiency. Moreover, these models can be integrated with advanced technological systems to create a highly efficient automated setup, enabling real-time monitoring of the drying process. Beyond their application to the drying kinetics of soursop, these models can also be employed to relatively predict the quality of products from other similar materials.

Acknowledgements: This study was supported by facilities provided by both Vingroup Innovation Fund (VinIF) and Nguyen Tat Thanh University, Ho Chi Minh City, Vietnam.

Funding information: Ngoc Duc Vu was funded by Master, PhD Scholarship Program of Vingroup Innovation Foundation (VINIF), code VINIF.2023.ThS.093 and Nguyen Tat Thanh University, Ho Chi Minh City, Vietnam provided with the facilities required to carry out this work.

Author contributions: H.B.L. and N.D.V.: conceptualization; N.D.V. and N.A.N.: data curation; N.D.V. and N.A.N.: formal analysis; N.D.V.: funding acquisition; N.D.V. and N.A.N.: investigation; N.D.V., N.A.N., and D.T.N.D.: methodology; N.D.V. and D.T.N.D.: project administration; N.D.V. and D.T.N.D.: resources; B.A.P. and N.D.V.: software; B.A.P., D.T.N.D., and N.D.V.: supervision; H.B.L. and N.D.V.: validation; B.A.P. and N.D.V.: visualization; B.A.P. and N.D.V.: writing – original draft; N.D.V.: writing – review and editing. All the authors agreed on the final version of the manuscript.

Conflict of interest: The authors declare that they have no conflicts of interest.

Ethical approval: The conducted research is not related to either human or animal use.

Data availability statement: All data generated or analyzed during this study are included in this published article.

References

[1] Pareek S, Yahia EM, Pareek OP, Kaushik RA. Postharvest physiology and technology of Annona fruits. Food Res Int. 2011;44:1741–51. doi: 10.1016/j.foodres.2011.02.016.

[2] Badrie N, Schauss AG. Soursop (*Annona muricata* L.): composition, nutritional value, medicinal uses, and toxicology. In Bioactive foods in promoting health. Amsterdam, The Netherlands: Elsevier; 2010. p. 621–43. doi: 10.1016/B978-0-12-374628-3.00039-6.

[3] Fernández AE, Obledo-Vazquez EN, Vivar-Vera MD, Ayerdi SG, Montalvo-Gonzalez E. Evaluation of emerging methods on the polyphenol content, antioxidant capacity and qualitative presence of acetogenins in soursop pulp (*Annona muricata* L.). Rev Bras Frutic. 2017;39:1–8. doi: 10.1590/0100-29452017358.

[4] Yajid AI, Ab Rahman HS, Wong MPK, Wan Zain WZ. Beneficios potenciales de Annona muricata en la lucha contra el cáncer: Una revisión. Malaysian. J Med Sci. 2018;25:5–15.

[5] Hajdu Z, Hohmann J. An ethnopharmacological survey of the traditional medicine utilized in the community of Porvenir, Bajo Paraguá Indian Reservation, Bolivia. J Ethnopharmacol. 2012;139:838–57. doi: 10.1016/j.jep.2011.12.029.

[6] Jaramillo MC, Arango GJ, González MC, Robledo SM, Velez ID. Cytotoxicity and antileishmanial activity of *Annona muricata* pericarp. Fitoterapia. 2000;71:183–6. doi: 10.1016/S0367-326X(99)00138-0.

[7] Vu ND, Doan TKL, Dao TP, Tran TYN, Nguyen NQ. Soursop fruit supply chains: Critical stages impacting fruit quality. J Agric Food Res. 2023;14:100754. doi: 10.1016/j.jafr.2023.100754.

[8] Atawodi S. Nigerian foodstuffs with prostate cancer chemopreventive polyphenols. Infect Agent Cancer. 2011;6:2–5. doi: 10.1186/1750-9378-6-S2-S9.

[9] Moghadamtousi SZ, Rouhollahi E, Hajrezaie M, Karimian H, Abdulla MA, Kadir HA. *Annona muricata* leaves accelerate wound healing in rats via involvement of Hsp70 and antioxidant defence. Int J Surg. 2015;18:110–7. doi: 10.1016/j.ijsu.2015.03.026.

[10] Medina I, Gallardo JM, González MJ, Lois S, Hedges N. Effect of molecular structure of phenolic families as hydroxycinnamic acids and catechins on their antioxidant effectiveness in minced fish muscle. J Agric Food Chem. 2007;55:3889–95. doi: 10.1021/jf063498i.

[11] Nguyen VT, Nguyen MT, Tran QT, Thinh PV, Bui LM, Le THN, et al. Effect of extraction solvent on total polyphenol content, total flavonoid content, and antioxidant activity of soursop seeds (*Annona muricata* L.). IOP Conf Ser Mater Sci Eng. 2020;736:1–6. doi: 10.1088/1757-899X/736/2/022063.

[12] Ampofo-Asiama J, Quaye B. The effect of pasteurisation on the microbiological and nutritional quality of soursop (*Annona muricata* L.) juice. Asian Food Sci J. 2018;6:1–8. doi: 10.9734/AFSJ/2019/45610.

[13] Del Carmen DR, Esguerra EB, Gerance AA. Consumer purchasing behavior for fresh soursop (*Annona muricata* L.): Evidence from Metro Manila and Calabarzon, Philippines. Philipp Agric Sci. 2020;103:132–9.

[14] Santos IL, Rodrigues AM, Amante ER, Silva LH. Soursop (*Annona muricata*) properties and perspectives for integral valorization. Foods. 2023;12:1448. doi: 10.3390/foods12071448.
[15] Siang LM, Ding P, Mohamed MTM. Response of 1-Methycyclopropene on postharvest quality of local soursop (*Annona muricata* L.). Sains Malaysiana. 2019;48:571–9. doi: 10.17576/jsm-2019-4803-09.
[16] Prabhakar H, Bock CH, Kerr WL, Kong F. Pecan color change during storage: kinetics and modeling of the processes. Curr Res Food Sci. 2022;5:261–71. doi: 10.1016/j.crfs.2022.01.015.
[17] Dao TP, Vu DN, Nguyen DV, Pham VT, Tran TYN. Study of jelly drying cashew apples (*Anacardium occidentale* L.) processing. Food Sci Nutr. 2022;10:363–73. doi: 10.1002/fsn3.2565.
[18] Keneni YG, Hvoslef-Eide AK, (Trine), Marchetti JM. Mathematical modelling of the drying kinetics of *Jatropha curcas* L. seeds. Ind Crop Prod. 2019;132:12–20. doi: 10.1016/j.indcrop.2019.02.012.
[19] Pal K, Asthana N, Aljabali AA, Bhardwaj SK, Kralj S, Penkova A, et al. A critical review on multifunctional smart materials 'nanographene' emerging avenue: nano-imaging and biosensor applications. Crit Rev Solid State Mater Sci. 2022;47:691–707. doi: 10.1080/10408436.2021.1935717.
[20] Patel KK, Kar A. Heat pump assisted drying of agricultural produce – an overview. J Food Sci Technol. 2012;49:142–60. doi: 10.1007/s13197-011-0334-z.
[21] Siqueira VC, Resende O, Chaves TH. Drying kinetics of jatropha seeds. Rev Ceres. 2012;59:171–7. doi: 10.1590/S0034-737X2012000200004.
[22] Goyal RK, Kingsly ARP, Manikantan MR, Ilyas SM. Thin-layer drying kinetics of raw mango slices. Biosyst Eng. 2006;95:43–9. doi: 10.1016/j.biosystemseng.2006.05.001.
[23] Salehi F, Kashaninejad M. Modeling of moisture loss kinetics and color changes in the surface of lemon slice during the combined infrared-vacuum drying. Inf Process Agric. 2018;5:516–23. doi: 10.1016/j.inpa.2018.05.006.
[24] Menges HO, Ertekin C. Mathematical modeling of thin layer drying of Golden apples. J Food Eng. 2006;77:119–25. doi: 10.1016/j.jfoodeng.2005.06.049.
[25] Thao BTT, Vo TTK, Tran TYN, Le DT, Tran TT, Bach LG, et al. Application of mathematical techniques to study the moisture loss kinetics and polyphenol degradation kinetics of mango (*Mangifera indica* L.) slices during heat pump drying by pilot equipment. LWT. 2023;176:114454. doi: 10.1016/j.lwt.2023.114454.
[26] Ramesh AM, Pal K, Kodandaram A, Manjula BL, Ravishankar DK, Gowtham HG, et al. Antioxidant and photocatalytic properties of zinc oxide nanoparticles phyto-fabricated using the aqueous leaf extract of *Sida acuta*. Green Process Synth. 2022;11:857–67. doi: 10.1515/gps-2022-0075.
[27] Watts SS, Pal K, Asthana N, Bhattu M, Verma M. Green synthesis by extraction of caffeine for cosmeceutical application: A review. J Mol Struct. 2024;1305:137733. doi: 10.1016/j.molstruc.2024.137733.
[28] Vu ND, Tran NTY, Le TD, Phan NTM, Doan PLA, Huynh LB, et al. Kinetic model of moisture loss and polyphenol degradation during heat pump drying of soursop fruit (*Annona muricata* L.). Processes. 2022;10:2082. doi: 10.3390/pr10102082.
[29] Taiwo A, Oboho E, Michael O. Investigation into the thin layer drying models of Nigerian popcorn varieties. Leonardo Electron J Pract Technol. 2008;7:47–62.
[30] Aghbashlo M, Kianmehr MH, Khani S, Ghasemi M. Mathematical modelling of thin-layer drying of carrot. Int Agrophys. 2009;23:313–7.
[31] Balbay A, Şahin Ö. Microwave drying kinetics of a thin-layer liquorice root. Dry Technol. 2012;30:859–64. doi: 10.1080/07373937.2012.670682.
[32] Laohavanich J, Wongpichet S. Thin layer drying model for gas-fired infrared drying of paddy. Songklanakarin J Sci Technol. 2008;30:343–8.
[33] Hii CL, Law CL, Cloke M. Modeling of thin layer drying kinetics of cocoa beans during artificial and natural drying. J Eng Sci Technol. 2008;3:1–10.
[34] Demir V, Gunhan T, Yagcioglu AK. Mathematical modelling of convection drying of green table olives. Biosyst Eng. 2007;98:47–53. doi: 10.1016/j.biosystemseng.2007.06.011.
[35] Akar G, Barutçu Mazı I. Color change, ascorbic acid degradation kinetics, and rehydration behavior of kiwifruit as affected by different drying methods. J Food Process Eng. 2019;42:e13011. doi: 10.1111/jfpe.13011.
[36] Yaldiz O, Ertekin C, Uzun HI. Mathematical modeling of thin layer solar drying of sultana grapes. Energy. 2001;26:457–65. doi: 10.1016/S0360-5442(01)00018-4.
[37] Ertekin C, Heybeli N. Thin-layer infrared drying of mint leaves. J Food Process Preserv. 2014;38:1480–90. doi: 10.1111/jfpp.12107.
[38] Doymaz I. Sun drying of figs: an experimental study. J Food Eng. 2005;71:403–7.
[39] Kumar N, Sarkar BC, Sharma HK. Mathematical modelling of thin layer hot air drying of carrot pomace. J Food Sci Technol. 2012;49:33–41. doi: 10.1007/s13197-011-0266-7.
[40] Degirmencioglu A, Yagcioglu K, Cagatay F. Drying characteristics of laurel leaves under different drying conditions. 7th International Congress on agricultural mechanization and energy, Adana; 1999. p. 565–9.
[41] Shah SB, Joshi MA. Modeling microwave drying kinetics of sugarcane bagasse. Int J Electron Eng. 2010;2(1):159–63.
[42] Midilli A, Kucuk H, Yapar Z. A new model for single-layer drying. Dry Technol. 2002;20:1503–13. doi: 10.1081/DRT-120005864.
[43] Karathanos VT. Determination of water content of dried fruits by drying kinetics. J Food Eng. 1999;39:337–44. doi: 10.1016/S0260-8774(98)00132-0.
[44] Diamante LM, Munro PA. Mathematical modelling of the thin layer solar drying of sweet potato slices. Sol Energy. 1993;51:271–6. doi: 10.1016/0038-092X(93)90122-5.
[45] Praveen Kumar DG, Hebbar HU, Ramesh MN. Suitability of thin layer models for infrared–hot air-drying of onion slices. LWT – Food Sci Technol. 2006;39:700–5. doi: 10.1016/j.lwt.2005.03.021.
[46] Lewis WK. The rate of drying of solid materials. J Ind Eng Chem. 1921;13:427–32. doi: 10.1021/ie50137a021.
[47] Roman MC, Fabani MP, Luna LC, Feresin GE, Mazza G, Rodriguez R. Convective drying of yellow discarded onion (Angaco INTA): Modelling of moisture loss kinetics and effect on phenolic compounds. Inf Process Agric. 2020;7:333–41. doi: 10.1016/j.inpa.2019.07.002.
[48] Page GE. Factors influencing the maximum rates of air drying shelled corn in thin layers. West Lafayette, Indiana: Purdue University; 1949.
[49] da Silva WP, e Silva CM, Farias VSO, Gomes JP. Diffusion models to describe the drying process of peeled bananas: Optimization and simulation. Dry Technol. 2012;30:164–74. doi: 10.1080/07373937.2011.628554.
[50] Diamante LM, Munro PA. Mathematical modelling of hot air drying of sweet potato slices. Int J Food Sci Technol. 1991;26:99–109. doi: 10.1111/j.1365-2621.1991.tb01145.x.

[51] Singh F, Katiyar VK, Singh BP. Mathematical modeling to study drying characteristic of apple and potato. International Conference on Chemical, Environment & Biological Sciences (CEBS-2014). Kuala Lumpur; 2014. p. 172–7.
[52] Thompson TL, Peart RM, Foster GH. Mathematical simulation of corn drying a new model. Trans ASAE. 1968;11:0582–6. doi: 10.13031/2013.39473.
[53] Henderson SM. Progress in developing the thin layer drying equation. Trans ASAE. 1974;17:1167–8. doi: 10.13031/2013.37052.
[54] Barroca MJ, Guiné R. Study of drying kinetics of quince. International Conference of Agricultural Engineering CIGR-AgEng2012; 2012.
[55] Verma LR, Bucklin RA, Endan JB, Wratten FT. Effects of drying air parameters on rice drying models. Trans ASAE. 1985;28:296–301. doi: 10.13031/2013.32245.
[56] Murthy DNP, Xie M, Jiang R. Weibull models. Hoboken, New Jersey: John Wiley & Sons; 2004.
[57] Udomkun P, Nagle M, Argyropoulos D, Mahayothee B, Latif S, Müller J. Compositional and functional dynamics of dried papaya as affected by storage time and packaging material. Food Chem. 2016;196:712–9. doi: 10.1016/j.foodchem.2015.09.103.
[58] Jha AK, Sit N. Drying characteristics and kinetics of colour change and degradation of phytocomponents and antioxidant activity during convective drying of deseeded Terminalia chebula fruit. J Food Meas Charact. 2020;14:2067–77. doi: 10.1007/s11694-020-00454-9.
[59] Uslu Demir H, Atalay D, Erge HS. Kinetics of the changes in bioactive compounds, antioxidant capacity and color of Cornelian cherries dried at different temperatures. J Food Meas Charact. 2019;13:2032–40. doi: 10.1007/s11694-019-00124-5.
[60] Ghanem Romdhane N, Bonazzi C, Kechaou N, Mihoubi NB. Effect of air-drying temperature on kinetics of quality attributes of lemon (Citrus limon cv. lunari) peels. Dry Technol. 2015;33:1581–9. doi: 10.1080/07373937.2015.1012266.
[61] Guiné RPF, Barroca MJ, Gonçalves FJ, Alves M, Oliveira S, Correia PMR. Effect of drying on total phenolic compounds, antioxidant activity, and kinetics decay in pears. Int J Fruit Sci. 2015;15:173–86. doi: 10.1080/15538362.2015.1017073.
[62] Niamnuy C, Devahastin S, Soponronnarit S, Vijaya Raghavan GS. Kinetics of astaxanthin degradation and color changes of dried shrimp during storage. J Food Eng. 2008;87:591–600. doi: 10.1016/j.jfoodeng.2008.01.013.
[63] Zarein M, Samadi SH, Ghobadian B. Investigation of microwave dryer effect on energy efficiency during drying of apple slices. J Saudi Soc Agric Sci. 2015;14:41–7.
[64] Jeevarathinam G, Pandiselvam R, Pandiarajan T, Preetha P, Krishnakumar T, Balakrishnan M, et al. Design, development, and drying kinetics of infrared-assisted hot air dryer for turmeric slices. J Food Process Eng. 2022;45:e13876. doi: 10.1111/jfpe.13876.
[65] Sacilik K, Elicin AK. The thin layer drying characteristics of organic apple slices. J Food Eng. 2006;73:281–9. doi: 10.1016/j.jfoodeng.2005.03.024.
[66] Royen MJ, Noori AW, Haydary J. Experimental Study and Mathematical Modeling of Convective Thin-Layer Drying of Apple Slices. Processes. 2020;8:1562. doi: 10.3390/pr8121562.
[67] Song X-D, Mujumdar AS, Law C-L, Fang X-M, Peng W-J, Deng L-Z, et al. Effect of drying air temperature on drying kinetics, color, carotenoid content, antioxidant capacity and oxidation of fat for lotus pollen. Dry Technol. 2020;38:1151–64. doi: 10.1080/07373937.2019.1616752.
[68] Abano EE, Ma H, Qu W. Influence of air temperature on the drying kinetics and quality of tomato slices. J Food Process Technol. 2011;2:1000123. doi: 10.4172/2157-7110.1000123.
[69] Onwude DI, Hashim N, Janius RB, Nawi NM, Abdan K. Modeling the thin-layer drying of fruits and vegetables: a review. Compr Rev Food Sci Food Saf. 2016;15:599–618. doi: 10.1111/1541-4337.12196.
[70] Nguyen TVL, Nguyen QD, Nguyen PBD. Drying kinetics and changes of total phenolic content, antioxidant activity and color parameters of mango and avocado pulp in refractance window drying. Pol J Food Nutr Sci. 2022;72:27–38. doi: 10.31883/pjfns/144835.
[71] Khiya Z, Oualcadi Y, Gamar A, Berrekhis F, Zair T, Hilali FEL. Correlation of total polyphenolic content with antioxidant activity of hydromethanolic extract and their fractions of the Salvia officinalis leaves from different regions of Morocco. J Chem. 2021;2021:1–11.
[72] López-Vidaña EC, Pilatowsky Figueroa I, Cortés FB, Rojano BA, Navarro Ocaña A. Effect of temperature on antioxidant capacity during drying process of mortiño (*Vaccinium meridionale* Swartz). Int J Food Prop. 2017;20:294–305. doi: 10.1080/10942912.2016.1155601.
[73] González EM, Fernández AE, Sáyago-Ayerdi SG, Estrada RM, Vallejo LG. In vitro antioxidant capacity of crude extracts and acetogenin fraction of soursop fruit pulp. Pharm Anal Acta. 2016;7:1–7. doi: 10.4172/2153-2435.1000484.
[74] Başlar M, Karasu S, Kiliçli M, Us AA, Saꞓdiç O. Degradation kinetics of bioactive compounds and antioxidant activity of pomegranate arils during the drying process. Int J Food Eng. 2014;10:839–48. doi: 10.1515/ijfe-2014-0080.
[75] Singhal S, Rasane P, Kaur S, Singh J, Gupta N. Thermal degradation kinetics of bioactive compounds in button mushroom (*Agaricus bisporus*) during tray drying process. J Food Process Eng. 2020;43:e13555. doi: 10.1111/jfpe.13555.
[76] Day AJ, Mellon F, Barron D, Sarrazin G, Morgan MRA, Williamson G. Human metabolism of dietary flavonoids: Identification of plasma metabolites of quercetin. Free Radic Res. 2001;35:941–52. doi: 10.1080/10715760100301441.
[77] Liu Y, Tikunov Y, Schouten RE, Marcelis LFM, Visser RGF, Bovy A. Anthocyanin biosynthesis and degradation mechanisms in solanaceous vegetables: a review. Front Chem. 2018;6:1–17. doi: 10.3389/fchem.2018.00052.
[78] Enaru B, Dreţcanu G, Pop TD, Stănilă A, Diaconeasa Z. Anthocyanins: Factors affecting their stability and degradation. Antioxidants. 2021;10:1967. doi: 10.3390/antiox10121967.
[79] Stagos D, Portesis N, Spanou C, Mossialos D, Aligiannis N, Chaita E, et al. Correlation of total polyphenolic content with antioxidant and antibacterial activity of 24 extracts from Greek domestic Lamiaceae species. Food Chem Toxicol. 2012;50:4115–24.
[80] Arslan D, Özcan MM. Drying of tomato slices: Changes in drying kinetics, mineral contents, antioxidant activity and color parameters. CYTA – J Food. 2011;9:229–36. doi: 10.1080/19476337.2010.522734.
[81] Sim YY, Nyam KL. Effect of different drying methods on the physical properties and antioxidant activities of Hibiscus cannabinus leaves. J Food Meas Charact. 2019;13:1279–86. doi: 10.1007/s11694-019-00043-5.
[82] Shin HY, Kim H, Jung S, Jeong EJ, Lee KH, Bae YJ, et al. Interrelationship between secondary metabolites and antioxidant capacities of Centella asiatica using bivariate and multivariate correlation analyses. Appl Biol Chem. 2021;64:82. doi: 10.1186/s13765-021-00656-9.